Spin waves in $CuFeO_2$

Randy S. Fishman[a)]
Materials Science and Technology Division, Oak Ridge National Laboratory, Oak Ridge, Tennessee 37831-6065, USA

(Presented on 8 November 2007; received 15 August 2007; accepted 30 October 2007; published online 11 February 2008)

One of the most fascinating frustrated antiferromagnets, $CuFeO_2$, contains stacked hexagonal layers, each with an $\uparrow\uparrow\downarrow\downarrow$ magnetic structure. Recent neutron-scattering studies have found that the spin-wave spectrum softens with increasing magnetic field or by substituting Al for Fe. We present a theory of the spin-wave excitations that fits the observed frequencies quite well and explains this softening. © *2008 American Institute of Physics*. [DOI: 10.1063/1.2834428]

Due to antiferromagnetic interactions between nearest neighbors within each hexagonal layer, $CuFeO_2$ provides one of the best examples of a geometrically frustrated antiferromagnet. Like other geometrically frustrated antiferromagnets,[1] $CuFeO_2$ supports competing ground states that depend sensitively on the exchange interactions and anisotropy. In this paper, we study the relation between the spin-wave excitations and the transformation between ground states in Al-doped $CuFeO_2$.

In zero field below 10.5 K, the $S=\frac{5}{2}$ Fe^{3+} spins of $CuFeO_2$ are found to order along the z axis in the $\uparrow\uparrow\downarrow\downarrow$ spin configuration[2,3] shown in Fig. 1(a). At low temperature, the spins are completely aligned with $\langle S_{iz}\rangle=\pm\frac{5}{2}$. Despite the apparent "Ising-like" character of the Fe^{3+} spins, inelastic neutron-scattering reveals that the spin-waves (SWs) are actually quite soft with an energy gap of only about 0.9 meV on either side of the ordering wavevector $\mathbf{Q}$.[4,5] The SW gap is found to decrease either with applied field along the z axis or by substituting nonmagnetic Al^{3+} ions for Fe^{3+}. At a critical Al concentration of about 1.6% (Ref. 4) or a critical magnetic field of about 7 T,[6] the SW gaps vanish, the spin structures become noncollinear,[7] and the crystals display multiferroic behavior.[6]

Takagi and Mekata[8] used mean-field theory to compare the ground-state energies of different possible two-dimensional, Ising-like spin configurations (all spins in the $\pm\hat{\mathbf{z}}$ directions) with the nearest-neighbor antiferromagnetic exchange $J_1<0$ and the next-nearest and next-next-nearest neighbor interactions J_2 and J_3 within each hexagonal plane, as shown in Fig. 1(a). They concluded that the $\uparrow\uparrow\downarrow\downarrow$ spin state is stable within the region of $\{J_2/|J_1|, J_3/|J_1|\}$ phase space sketched in Fig. 1(b), bordered by the dashed lines and extending down to $J_3/|J_1|=-\infty$. Assuming that adjacent hexagonal planes are stacked antiferromagnetically, then the nearest-neighbor antiferromagnetic coupling J_z along the z axis and the single-ion anisotropy $-D\Sigma_i S_{iz}^2$ on every site do not affect this phase diagram since the energy of each Ising-like phase is changed by the same amount. However, those terms are essential to accurately describe the spin dynamics of the $\uparrow\uparrow\downarrow\downarrow$ phase in $CuFeO_2$.

The Hamiltonian of $CuFeO_2$ in a magnetic field $\mathbf{B}=B\hat{\mathbf{z}}$ along the $+\hat{\mathbf{z}}$ direction is simply given by

$$H=-\frac{1}{2}\sum_{i\neq j}J_{ij}\mathbf{S}_i\cdot\mathbf{S}_j-D\sum_i S_{iz}^2-g\mu_B B\sum_i S_{iz}, \tag{1}$$

where $J_{ij}=J_1$, J_2, J_3, or J_z, depending on the relative vector $\mathbf{R}_i-\mathbf{R}_j$ between sites i and j. Although the actual magnetic unit cell of $CuFeO_2$ sketched in Ref. 5 contains six hexagonal layers, we assume a simplified crystal with only two layers per magnetic unit cell and adjacent layers stacked one on top of the other antiferromagnetically. This reduces the number of inequivalent spins per unit cell from 12 to 4, allowing us to provide an analytic expression for the SW frequencies. Despite this simplification, the evaluated SW dispersion along the q_z axis agrees quite well with inelastic neutron-scattering measurements, as shown elsewhere.[5] In a further simplification, we ignore the very small ($<0.4\%$) distortion of the hexagonal plane[9] that reduces the energy of one of the three $\uparrow\uparrow\downarrow\downarrow$ phases with respect to the other two. While this magnetoelastic distortion may be significant for other properties, it changes the SW dynamics only very slightly.

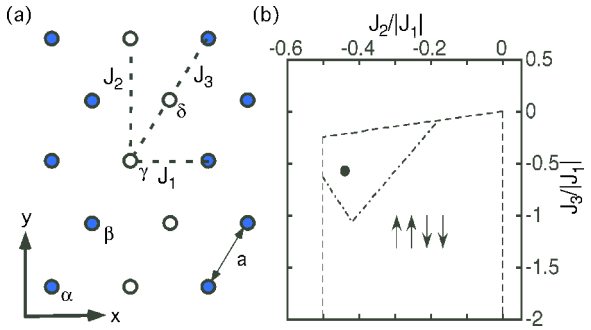

FIG. 1. (Color online) (a) The spin arrangement (up spins are filled and down spins are empty circles) of $CuFeO_2$ in each hexagonal plane, with the exchange parameters J_1, J_2, and J_3 and the four inequivalent spins α, β, γ, and δ. (b) The region in $\{J_2/|J_1|, J_3/|J_1|\}$ phase space (with $J_1<0$) where the $\uparrow\uparrow\downarrow\downarrow$ phase is stable (Ref. 8) against other "Ising-like" phases is bordered by the dashed lines and extends down to $J_3/|J_1|=-\infty$. A fit to the observed SW frequencies (Ref. 5) gives the solid point. When $D/|J_1|=0.2$, the $\uparrow\uparrow\downarrow\downarrow$ phase is locally stable only within the smaller region bordered by the dashed and dash-dotted lines.

a)Electronic mail: fishmanrs@ornl.gov

For the spin configuration shown in Fig. 1(a), the antiferromagnetic ordering wavevector is given by $\mathbf{Q}=(\pi/a,0,\pi/c)$, where $a\approx 3.04$ Å is the nearest-neighbor distance in each plane and $c\approx 2a$ is the separation between adjacent hexagonal planes. In the reference frames defined by the primitive real-space translation vectors $\mathbf{e}_1=(a/2)\hat{\mathbf{x}}+(\sqrt{3}a/2)\hat{\mathbf{y}}$, $\mathbf{e}_2=(a/2)\hat{\mathbf{x}}-(\sqrt{3}a/2)\hat{\mathbf{y}}$, and $\mathbf{e}_3=3c\hat{\mathbf{z}}$ and the corresponding reciprocal-lattice vectors, $\mathbf{Q}$ corresponds to the wavevector $[\frac{1}{4},\frac{1}{4},\frac{3}{2}]$.

Employing a Holstein-Primakoff $1/S$ expansion about the classical limit, we express the spins $\mathbf{S}_i$ on the inequivalent sites α, β, γ, and δ in terms of the boson operators α_i, β_i, γ_i, and δ_i. To first order in $1/S$, the Fourier-transformed Hamiltonian can then be written as

$$H = E_0 + \sum_{\mathbf{q}} \{A(\mathbf{q})^{(+)}(\alpha_{\mathbf{q}}^{\dagger}\alpha_{\mathbf{q}} + \beta_{\mathbf{q}}^{\dagger}\beta_{\mathbf{q}}) + A(\mathbf{q})^{(-)}(\gamma_{\mathbf{q}}^{\dagger}\gamma_{\mathbf{q}} + \delta_{\mathbf{q}}^{\dagger}\delta_{\mathbf{q}}) + C(\mathbf{q})(\alpha_{\mathbf{q}}\gamma_{\mathbf{q}} + \alpha_{\mathbf{q}}^{\dagger}\gamma_{\mathbf{q}}^{\dagger} + \beta_{\mathbf{q}}\delta_{\mathbf{q}} + \beta_{\mathbf{q}}^{\dagger}\delta_{\mathbf{q}}^{\dagger}) + D(\mathbf{q})(\alpha_{\mathbf{q}}^{\dagger}\beta_{\mathbf{q}} + \delta_{\mathbf{q}}^{\dagger}\gamma_{\mathbf{q}} + \delta_{\mathbf{q}}\alpha_{\mathbf{q}} + \beta_{\mathbf{q}}^{\dagger}\gamma_{\mathbf{q}}^{\dagger}) + D(\mathbf{q})^{\star}(\beta_{\mathbf{q}}^{\dagger}\alpha_{\mathbf{q}} + \gamma_{\mathbf{q}}^{\dagger}\delta_{\mathbf{q}} + \delta_{\mathbf{q}}^{\dagger}\alpha_{\mathbf{q}}^{\dagger} + \beta_{\mathbf{q}}\gamma_{\mathbf{q}})\}, \tag{2}$$

where $E_0\sim S^2$ is the mean-field energy, $A(\mathbf{q})^{(\pm)}=A(\mathbf{q})\pm g\mu_B B$, and

$$A(\mathbf{q}) = 2S\{D - J_1 + J_2[1-\cos(q_y\sqrt{3}a)] - J_3[1+\cos(2q_x a)] - J_z\}, \tag{3}$$

$$C(\mathbf{q}) = -2S\{J_1 + 2J_3\cos(q_y\sqrt{3}a)\}\cos(q_x a) - 2SJ_z\cos(q_z c), \tag{4}$$

$$D(\mathbf{q}) = -2S\cos(q_y\sqrt{3}a/2)\{J_1 e^{iq_x a/2} + J_2 e^{-3iq_x a/2}\}. \tag{5}$$

Notice that the $\{\alpha,\beta,\gamma,\delta\}$ spins in one hexagonal layer are coupled by the nearest-neighbor exchange J_z to the $\{\gamma,\delta,\alpha,\beta\}$ spins in adjacent layers.

Diagonalizing the Hamiltonian H is equivalent to solving two sets of coupled equations of motion. The first set for $\mathbf{v}_{\mathbf{q}}=(\alpha_{\mathbf{q}},\beta_{\mathbf{q}},\gamma_{\mathbf{q}}^{\dagger},\delta_{\mathbf{q}}^{\dagger})$ may be written in matrix form as $id\mathbf{v}_{\mathbf{q}}/dt=-[H,\mathbf{v}_{\mathbf{q}}]=\underline{M}(\mathbf{q})\mathbf{v}_{\mathbf{q}}$, where the 4×4 matrix $\underline{M}(\mathbf{q})$ is given by

$$\underline{M}(\mathbf{q}) = \begin{pmatrix} A(\mathbf{q})^{(+)} & D(\mathbf{q}) & C(\mathbf{q}) & D(\mathbf{q})^{\star} \\ D(\mathbf{q})^{\star} & A(\mathbf{q})^{(+)} & D(\mathbf{q}) & C(\mathbf{q}) \\ -C(\mathbf{q}) & -D(\mathbf{q})^{\star} & -A(\mathbf{q})^{(-)} & -D(\mathbf{q}) \\ -D(\mathbf{q}) & -C(\mathbf{q}) & -D(\mathbf{q})^{\star} & -A(\mathbf{q})^{(-)} \end{pmatrix}. \tag{6}$$

The SW frequencies are then determined from the condition $\mathrm{Det}[\underline{M}(\mathbf{q})-\epsilon(\mathbf{q})\underline{I}]=0$ or

$$[\epsilon(\mathbf{q}) - g\mu_B B]^2 = A(\mathbf{q})^2 - C(\mathbf{q})^2 \pm \{[D(\mathbf{q})^2 - D(\mathbf{q})^{\star 2}]^2 + 4|A(\mathbf{q})D(\mathbf{q}) - C(\mathbf{q})D(\mathbf{q})^{\star}|^2\}^{1/2}. \tag{7}$$

The second set of coupled equations of motion for $\mathbf{v}_{\mathbf{q}}^{\dagger}$ gives the same expression but with a + sign before the $g\mu_B B$ term on the left. Hence, each of the SW branches is linearly split by $\pm g\mu_B B$, as expected for an antiferromagnet.

As shown in Ref. 5, the parameters that provide the best fit to the neutron-scattering data in zero field are $J_1S=-1.14$ meV, $J_2S=-0.50$ meV, $J_3S=-0.65$ meV, $J_zS=-0.33$ meV, and $DS=0.17$ meV. These values produce the two upper SW modes plotted in Fig. 2 as the solid and dashed curves. The q_x axis has been scaled so that the ordering wavevector $\mathbf{Q}$ lies at the $\frac{1}{4}$ point. Notice that the SW gap of about 0.9 meV occurs at wavevectors $\mathbf{q}^{(\pm)}=[(1\pm 0.18)\pi/a,0,\pi/c]$ on either side of $\mathbf{Q}$, as found experimentally.[4,5] Since the SW branches are linearly split in a magnetic field, our results imply that the critical field required to destabilize the $\uparrow\uparrow\downarrow\downarrow$ phase is $B_c=0.9$ meV$/2\mu_B\approx 7.7$ T, just slightly larger than the experimental value.[6]

The exchange parameters given above correspond to $J_2/|J_1|=-0.44$ and $J_3/|J_1|=-0.57$, which is denoted by the solid point in Fig. 1(b). Consequently, the $\uparrow\uparrow\downarrow\downarrow$ phase is stable against other Ising-like phases with spins aligned along the $\pm\hat{\mathbf{z}}$ directions. The local (but not global) stability of the $\uparrow\uparrow\downarrow\downarrow$ phase is guaranteed by the positive values of the SW frequencies for all $\mathbf{q}$. In the limit $D/|J_1|\to\infty$, the $\uparrow\uparrow\downarrow\downarrow$ phase is both globally stable against other Ising-like phases and locally stable against slight rotations of the spins (since all the SW frequencies would be infinite) in the whole region of Fig. 1(b) bordered by the dashed lines and extending down to $J_3/|J_1|=-\infty$. However, as $D/|J_1|$ decreases, the $\uparrow\uparrow\downarrow\downarrow$

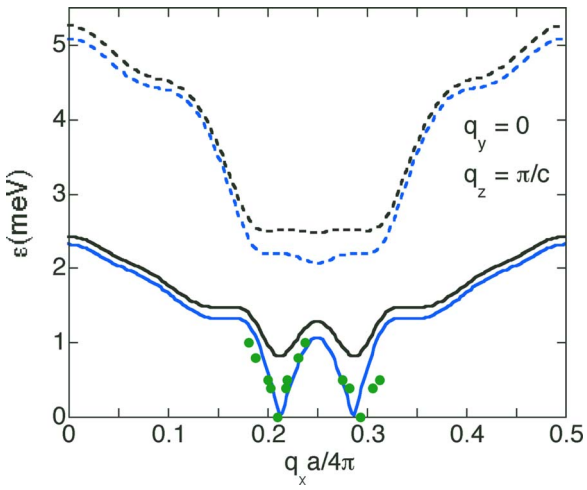

FIG. 2. (Color online) The SW frequencies along the q_x direction with $q_y=0$ and $q_z=\pi/c$. The solid and dashed curves denote the two SW branches for the exchange parameters given in the text. The upper solid and dashed curves are for anisotropy $DS=0.17$ meV and the lower for $DS=0.12$ meV. The measured SW frequencies for Al doping of 0.02 (Ref. 4) are plotted as the solid points.

phase remains locally stable within a shrinking region of $\{J_2/|J_1|, J_3/|J_1|\}$ phase space. For a given set $\{J_1, J_2, J_3\}$ of exchange parameters, the $\uparrow\uparrow\downarrow\downarrow$ phase becomes locally unstable when $D<D_c$ since the SW frequencies become negative near $\mathbf{q}^{(\pm)}$. For the exchange and anisotropy parameters given above, $DS=0.17$ meV and $D_cS=0.12$ meV. When $D/|J_1|=0.2$, the $\uparrow\uparrow\downarrow\downarrow$ phase is stable within the small region of Fig. 1(b) bordered by the dashed and dash-dotted lines, which contains the solid point. Since the lattice is not frustrated along the z direction, the value of J_z does not effect the boundaries for the stability of the $\uparrow\uparrow\downarrow\downarrow$ phase.

Doping with Al is found to soften the SW frequencies of $CuFe_{1-x}Al_xO_2$ at the same wavevectors $\mathbf{q}^{(\pm)}$ where the lower SW branch of pure $CuFeO_2$ has minima.[4] As shown in Fig. 2, reducing the SW anisotropy parameter DS from 0.17 meV to $D_cS=0.12$ meV provides a good fit to the the measured frequencies with an Al doping of $x=0.02$, slightly above the critical value of 0.016. Notice that both the measured and theoretical frequencies exhibit a linear dispersion about $\mathbf{q}^{(\pm)}$. Therefore, the dominant effect of swapping Fe^{3+} for Al^{3+} may be to suppress the single-ion anisotropy while keeping the other exchange parameters relatively unchanged. Though the present theory clearly indicates that the $\uparrow\uparrow\downarrow\downarrow$ phase becomes unstable when $B>B_c$ or when $D<D_c$, we have thus far been unable to determine the nature of the "noncollinear-incommensurate" phase[6,10] that is stable above 7 T or when the Al concentration exceeds 0.016.

The low value of the anisotropy parameter D implies that the Fe^{3+} moments can fluctuate much more readily than the Ising-like nature of their long-range order might suggest. Conversely, it is difficult to understand how Fe^{3+} ions with $S=\frac{5}{2}$ and $L=0$ can exhibit any magnetic anisotropy at all. One possibility is that due to oxidation, the admixture of $S=2$ Fe^{2+} impurities permits single-ion magnetic anisotropy D to develop. If the Al^{3+} dopants preferentially replace the Fe^{2+} rather than the Fe^{3+} ions, then they would have the effect of decreasing the anisotropy D. Hopefully, future experiments will confirm this hypothesis.

It is a pleasure to acknowledge helpful conversations with Prof. Mark Meisel and with Dr. Feng Ye and Dr. Jaime Fernandez-Baca, whose experiments motivated the current theoretical study. Research sponsored by the Division of Materials Science and Engineering of the U.S. Department of Energy.

[1]See, for example, *Frustrated Spin Systems* (World Scientific, New Jersey, 2004), edited by H. T. Diep.
[2]S. Mitsuda, H. Yoshizawa, N. Yaguchi, and M. Mekata, J. Phys. Soc. Jpn. **60**, 1885 (1991).
[3]M. Mekata, N. Yaguchi, T. Takagi, T. Sugino, S. Mitsuda, H. Yoshizawa, N. Hosoito, and T. Shinjo, J. Phys. Soc. Jpn. **12**, 4474 (1993).
[4]N. Terada, S. Mitsuda, Y. Oohara, H. Yoshizawa, and H. Takei, J. Magn. Magn. Mater. **272–276**, e997 (2004); N. Terada, S. Mitsuda, T. Fujii, and D. Petitgrand, J. Phys.: Condens. Matter **19**, 145241 (2007).
[5]F. Ye, J. A. Fernandez-Baca, R. S. Fishman, Y. Ren, H. J. Kang, Y. Qiu, and T. Kimura, Phys. Rev. Lett. **99**, 157201 (2007).
[6]T. Kimura, J. C. Lashley, and A. P. Ramirez, Phys. Rev. B **73**, 220401(R) (2006).
[7]O. A. Petrenko, M. R. Lees, G. Balakrishnan, S. de Brion, and G. Chouteau, J. Phys.: Condens. Matter **17**, 2741 (2005).
[8]T. Takagi and M. Mekata, J. Phys. Soc. Jpn. **64**, 4609 (1995).
[9]F. Ye, Y. Ren, Q. Huang, J. A. Fernandez-Baca, P. Dai, J. W. Lynn, and T. Kimura, Phys. Rev. B **73**, 220404(R) (2006).
[10]N. Terada, Y. Narumi, K. Katsumata, T. Yamamoto, U. Staub, K. Kindo, M. Hagiwara, Y. Tanaka, A. Kikkawa, H. Toyokawa, T. Fukui, R. Kanmuri, T. Ishikawa, and H. Kitamura, Phys. Rev. B **74**, 180404(R) (2006).